Water Induced Effects on the Thermal Response of a Protein

Simone Melchionna,[1] Giuseppe Briganti,[1] Paola Londei,[2] and Piero Cammarano[3]
[1]*Dipartimento di Fisica and INFM, Università "La Sapienza", Piazzale Aldo Moro 5, 00185 Rome, Italy*
[2]*Dipartimento di Biochimica Medica e Biologia Medica, Università di Bari, Piazzale Giulio Cesare, 70124, Bari, Italy*
[3]*Dipartimento di Biotecnologie Cellulari e Ematologia, Università "La Sapienza", Policlinico Umberto I, Viale Regina Elena 324, 00162, Rome, Italy*
(Received 30 July 2003; published 13 April 2004)

A model protein and surrounding water have been investigated at different temperatures. We have detected an anomalous compression of the protein near the freezing point of water—a compression not obviously related to the negative thermal expansion of the solvent. Moreover, the physiological protein working temperature ($T = 300$ K) appears to be related to the activation of exchange of vicinal water with the bulk and the concomitant absorption of heat by hydrophilic amino acids. The inferred activation was interpreted on the basis of degenerate tetrahedral order between the hydration shell and the bulk. The results support the notion that the dynamics of vicinal water makes a substantial contribution to the activity optimum of proteins.

DOI: 10.1103/PhysRevLett.92.158101 PACS numbers: 87.14.Ee, 82.60.–s, 82.70.–y, 87.15.Aa

Protein stability is affected by the composition and by the structural and thermodynamic states of the surrounding solvent. Water is a unique network-forming fluid entertaining both hydrophobic and highly specific interactions with proteins and inducing a conformational flexibility not seen in crystals or in nonaqueous environments [1,2]. Water induces the unfolding of certain proteins near the solvent freezing point. "Cold unfolding" takes place at relatively high pressures (>2 Kbar), while at lower pressures only destabilization occurs [3,4]. According to some, cold unfolding can be satisfactorily described by the equation of state of pure water ([5] and references therein) and the stabilization of large aggregates is favored when water approaches the liquid-vapor phase transition [6]. According to others, cold unfolding can be explained by the disruption at high pressure of water-water hydrogen bonds adjacent to the protein surface [7]. This situation suggests that investigating the protein-water interface may provide clues to understanding the mechanisms underlying the thermal stability of proteins [8].

We have employed molecular dynamics to study the thermal behavior of a protein domain [the guanosine triphosphate binding region of the *Escherichia coli* elongation factor Tu (EF-Tu) [9]] surrounded by 2929 water molecules. The hydrated protein has been studied at temperatures of $T = 240$, 255, 270, 285, 300, 330, 360, and 390 K and pressure of 1 atm. At each temperature, we initially equilibrated the system for 200 ps and subsequently simulated the system for 1 ns. The 1 ns interval could be insufficient to observe nonlocal conformational rearrangements, but it is long enough to study local motions for both the solute and the solvent. All observables employed in this work appeared stationary and no major conformational changes were observed during the runs. All simulations and analyses were performed with the DLPROTEIN simulation package [10].

The Charmm22 force field models the protein interatomic forces [11], and the consistent TIP3P models water [12]. Alternatively, other force fields could be employed to model hydrated proteins which could provide more accurate results for the conformational distribution of proteins [13]. However, the Charmm22 force field is expected to accurately reproduce the protein-water interfacial properties as investigated in the present Letter. The energetics and the dielectric constant of the model (82) [14,15] are in good agreement with the experimental data. However, the diffusion and expansion coefficients are 2.2 and 3.6 times larger, respectively, than the experimental values, and a density maximum at $T = 260$ K instead of 278 K.

On preliminary studies, we analyzed the temperature dependence of the protein packing attitude (monitored via the Voronoi volume), the volume of the simulation cell, and the root mean square deviation (RMSD) of the protein from the x-ray positions [16] (Fig. 1). The hydrated *G* domain shows a nonmonotonic thermal expansion characterized by a significant compression of the protein volume at 255 K (about 50% the volume at 270 K) and by fluctuations considerably larger (about 50%) than those seen at 285 and 255 K. Below 255 K, the protein expands again and the anomaly in the fluctuations disappears. Above 255 K, both the protein volume and the fluctuations are monotonic and can be categorized as solidlike thermal expansions. The apparent compression of the protein at low temperature is mirrored in the RMSD of the protein structure from the corresponding x-ray structure. As Fig. 1 shows, the RMSD displays a minimum at 255 K followed by a smooth increase over the 255–300 K range, and by a plateau between 300 and 330 K, indicating a range of marginal structural stability. At $T > 330$ K, the RMSD displays a steep rise reflecting the onset of protein unfolding.

The system excess volume (shown in the Fig. 1, inset) provides an estimate of the protein-solvent average

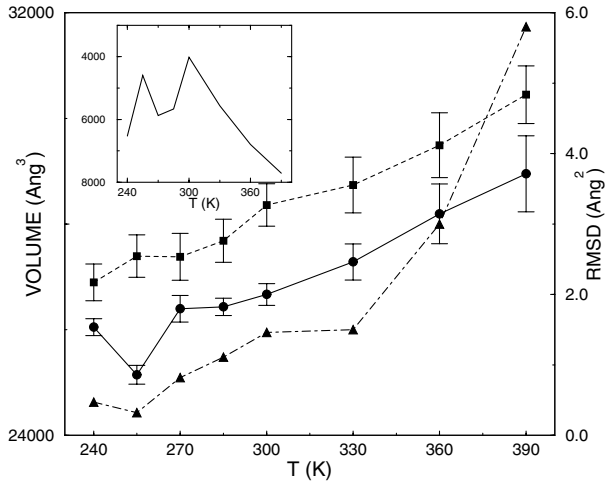

FIG. 1. Protein volume (circles), cell volume divided by four (squares), and root mean square displacement (triangles) versus temperature. The bars on the protein and cell volumes refer to their fluctuations. Inset: protein excess volume (see text).

interactions reflecting the deviation of the mixture from the ideal behavior. Usually, the excess volume is defined as the difference between the volume of the interacting mixture and the volume of the reference components. For our system, a reference state for the protein cannot be clearly defined. Therefore, we assign all the excess properties to the solvent whose reference state is the bulk. Under these assumptions, the excess volume is defined $V^{\mathrm{ex}} = V - V^{\mathrm{prot}} - n^W v^W$, where V is the volume of the simulation cell, V^{prot} is the protein volume in solution, n^W is the number of water molecules surrounding the protein, and v^W is the molecular volume of TIP3P bulk water. Values are negative at all temperatures due to the predominantly attractive water-solute interactions with distinct minima at 255 and 300 K. One could speculate that the protein compression at 255 K is accounted for by the expansion of water in the vicinity of the freezing point. We separately investigated the temperature dependence of the molecular volume of bulk water and found that, between 255 and 270 K, TIP3P water has a negative thermal expansion coefficient (about $3 \times 10^{-6}\ \mathrm{K}^{-1}$) significantly smaller than the experimental value ($2.53 \times 10^{-4}\ \mathrm{K}^{-1}$). Most probably, the discrepancy reflects the difficulty of generating a "good" ice crystal over the simulated time interval of 200 ps. On the other hand, the experimental expansion of water correlates well with the concomitant protein contraction. The fact that the simulation cell in Fig. 1 does not show the same shrinking as the protein volume could be ascribed to the presence of inhomogeneus regions around the macromolecule, or to a crystal order of water larger than that of the bulk—a condition possibly triggered by the protein acting as a nucleation center.

We next investigated the tetrahedral order of the water molecules comprising a shell of 3 Å around the protein. The tetrahedral arrangement in the first four neighbors around a given water molecule is evaluated via the parameter $S_g = 1 - \frac{3}{8}\sum_{j=1,3}\sum_{k=j+1,4}(\cos\psi_{jik} + \frac{1}{3})^2$, where ψ_{jik} is the angle formed between two neighboring atoms j and k and the oxygen atom of the central water molecule i [17,18]. All protein and water hydrogen bond donors and acceptors were assumed to be potential tetrahedral partners for a water molecule. S_g equals one when all angles are tetrahedral, and zero when the positions are uncorrelated.

Figure 2 shows the variation of the tetrahedral order parameter S_g for water molecules comprising bulk water [Fig. 2(a)] and the hydration shell [Fig. 2(b)] at three different temperatures. Apparently, bulk water exhibits two distinct behaviors. At low temperature, the S_g histogram is shifted to the right, due to a highly ordered structure in the ice arrangement, while a shoulder, whose height increases with temperature, appears at lower S_g. At higher temperatures, the shoulder develops into a maximum, indicating a decreased tetrahedral order in the liquid structure [18]. The transition between the two temperature regimes is found around 300 K, where the distribution is practically bimodal.

This condition may reflect an enhanced migration of the vicinal water molecules away from the protein surface. This latter hypothesis was substantiated by analyzing the number of water molecules residing for more than 50 ps in a 3 Å shell around the protein surface. The results, given in Table I, show that at $T = 240$ K a large number of water molecules lies within the hydration layer while, at $255 < T < 285$ K, their number drops by about one-third. Importantly, however, above $T = 300$ K less than 50% of the water molecules reside in the hydration layer for times longer than 50 ps. The behavior of the water molecules above 300 K is paralleled by a progressive drop of residence times, as the unfolding proceeds.

In order to determine whether the activation of exchange of vicinal water with the bulk reflects a

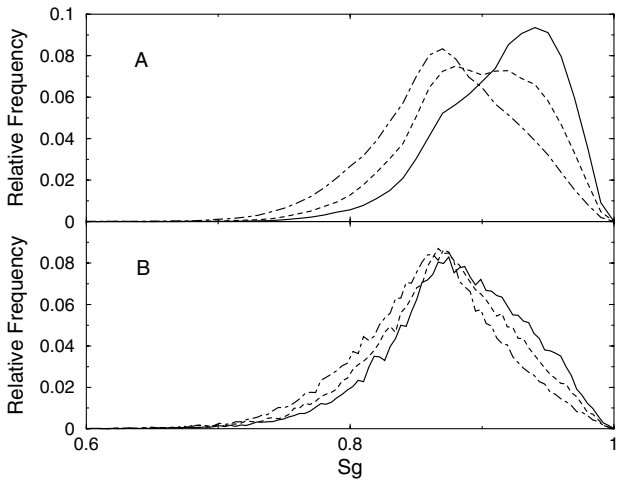

FIG. 2. Histograms of the tetrahedral order parameter of bulk water [panel (a)] and the hydration water in a layer of 3 Å around the protein surface [panel (b)] calculated at $T =$ 240 (solid line), 300 (dashed line), and 390 K (dot-dashed line).

TABLE I. Number of water molecules remaining in the shell of 3 Å around the protein for a time longer than 50 ps (ν), lifetimes (in ps) of protein-protein (τ_{hb}^{PP}), protein-water (τ_{hb}^{PW}), and water-water (τ_{hb}^{WW}) hydrogen bonds.

T (K)	ν	τ_{hb}^{PP}	τ_{hb}^{PW}	τ_{hb}^{WW}
240	71	37.09	4.16	10.06
255	52	29.61	3.66	8.024
270	45	20.19	3.14	6.32
285	42	16.60	2.82	5.19
300	29	10.93	2.55	4.40
330	26	8.95	2.28	3.27
360	9	5.62	2.05	2.62
390	8	4.43	1.88	2.16

microphase transition, we next investigated the chemical, electrostatic, and van der Waals contributions to the potential energy of polar and nonpolar amino acids. The chemical contribution refers to atoms covalently bonded within the protein as parametrized by the Charmm force field [11] and includes angular and torsional interactions. The energy values in Fig. 3 were summed over all atoms belonging to the two amino acid classes and include both protein-protein and protein-water interactions. The largest increase regards the chemical energies arising from wider fluctuations of atomic positions at short distances. Both the electrostatic contributions from nonpolar amino acids and the van der Waals contributions are generally small and increase smoothly with increasing temperature. The most important thermal variation of electrostatic energy arises from nonpolar amino acids. In particular, two separate linear regimes are apparent for the polar amino acids, with a transition temperature of 300 K associated with a jump in specific heat.

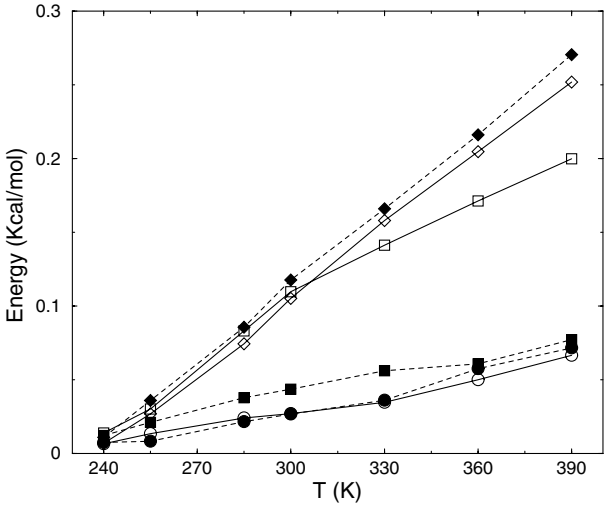

FIG. 3. Potential energies of amino acids, divided by polar (solid line and open symbols) and nonpolar (dashed line and filled symbols) classes, and by van der Waals (circles), electrostatic (squares), and chemical (diamonds) contributions. Each contribution has been shifted by an arbitrary value.

We next investigated the number of hydrogen bonds involving protein atoms, hydration water molecules, and bulk water molecules assuming that a hydrogen bond donor and acceptor are bonded if their relative distance is shorter than 3.5 Å and the donor-hydrogen-acceptor angle is larger than 150°. The number of hydrogen bonds, corresponding to protein-protein, protein-water, and water-water partners, is reported in Fig. 4. The contributions arising from hydration water molecules, bonded to other hydration water, to the protein, and to the bulk water, are illustrated in the figure inset. As Fig. 4 shows, the number of protein-water hydrogen bonds exhibits a quasilinear trend below $T = 330$ K, followed by a sudden increase at 360 K and by a decrease at 390 K. Correspondingly, the protein experiences a drop in the number of intramolecular hydrogen bonds above 330 K. Once again, the protein unfolds above 330 K, with a concomitant drop of protein-protein bonds and a rise of protein-solvent bonds.

In contrast to the quasilinear regime of water-protein hydrogen bonds, the low temperature protein-protein interactions display an irregular trend characterized by irregularities at 255 and 330 K. A comparison of intramolecular and intermolecular hydrogen bonds suggests a competition between protein-protein and protein-water partners. Below the freezing point of water, the protein-protein hydrogen bonds prevail and, surprisingly, the number of hydrogen bonds at $T = 255$ K is larger than that seen at $T = 240$ K. Above 270 K, the number of protein-protein bonds decays smoothly with increasing temperature, until unfolding occurs above 330 K.

A prominent feature of the results is the decrease of hydrogen bonds involving hydration water. At 255 K, the increase of protein-protein bonds is not paralleled by a

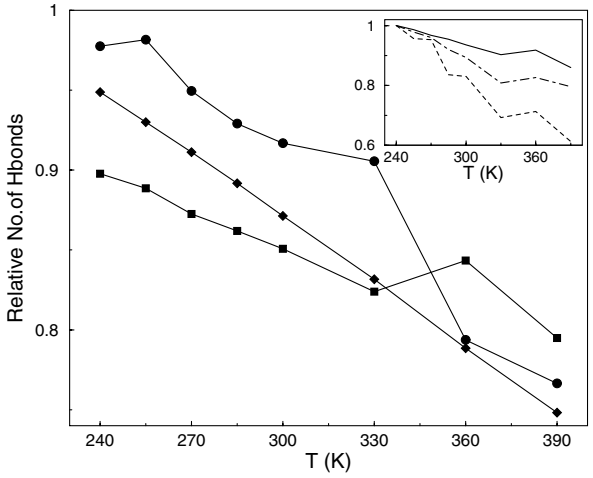

FIG. 4. Number of hydrogen bonds for protein-protein (circles), protein-water (squares), and water-water (diamonds) partners. The values have been divided by the number of hydrogen bonds found at $T = 0$ K, for each class of partners. Inset: number of hydrogen bonds grouped by protein-hydration water (solid line), hydration water-hydration water (dashed line), and hydration water-bulk water (dot-dashed line).

concomitant decrease of the protein-hydration water bonds. Instead, a depletion of bonds occurs between molecules comprising the same hydration shell, as expected if the hydration water closely follows the remodelling of the protein surface. Moreover, water molecules in the hydration shell form the strongest hydrogen bonds when bonded to the protein, and the weakest bonds when bonded among themselves. This implies that the protein static disorder inhibits hydration water from generating a substantial number of intrashell links.

For bulk water, the hydrogen bond lifetimes fit an Arrhenius-like decay with an activation energy of 1.9 kcal/mol (data not shown). For the hydrated protein, the Arrhenius plot indicates activation energies of 2.6 kcal/mol for the protein-protein hydrogen bonds, and 1.0 kcal/mol for the protein-water hydrogen bonds. On the whole, protein-protein hydrogen bonds show a higher degree of thermal stability than either protein-water or water-water bonds. Protein-water bonds exhibit short lifetimes and low activation energies indicating that their breakage is caused by the rototranslational motion of the water partners. Moreover, their weakness correlates well with the low tetrahedrality (see Fig. 2) and amorphous structure of vicinal water, and the tendency of water molecules to easily escape from the hydration shell at high temperature.

In summary, the most prominent feature of the low T regime (<300 K) is a "compression" of the EF-Tu G domain near the freezing point of bulk water. This phenomenon is consistent with three lines of evidence. First, the mixture excess volume shows a minimum at $T = 255$ K. Second, the number of protein-hydration water hydrogen bonds decreases linearly with temperature between $240 < T < 330$ K. Third, different experimental results point towards this direction. X-ray analysis of myoglobin crystals show a nonuniform and anisotropic thermal expansion, mostly contributed by the expansion of small, subatomic free volumes [19]. Inelastic neutron scattering and infrared spectroscopy revealed that the protein atoms undergo a discontinuity at 250 K and hydration water does not exhibit the negative thermal expansion coefficient found in bulk water [20]. On the whole, the available data suggest that the protein contraction is due to a preference of protein-protein over protein-water hydrogen bonds, accompanied by a reshaping of the hydration shell. Moreover, nonuniform and inhomogenous regions in the proximity of the protein surface can be responsible for keeping the two subsystems in weak interaction. Our results confirm the observation that at low temperatures hydration water displays an amorphous structure and acts as a plastic buffer to protect the biomolecule against mechanical stress.

The high temperature regime (>300 K) reveals two interesting features. One is a quasi-ideal behavior of the protein volume at 300 K, where we detected the smallest excess volume and the highest number of protein-protein hydrogen bonds. The other is a range of marginal stability between $300 < T < 330$ K. Above 330 K, water progressively infiltrates the protein structure until unfolding occurs.

The tetrahedral order found for TIP3P bulk water strongly resembles the results obtained for SPC/E bulk water [18], as well as energetics is usually well captured by these models, suggesting that the properties of vicinal water are rather independent on the employed model. Around 300 K, the observed degeneracy of orientational states between vicinal and bulk water and the concomitant decrease of "residence times" is related to the electrostatic contribution to specific heat arising from hydrophilic amino acids. The activation of exchange of vicinal water corresponds to the physiological optimum of the protein.

The authors are grateful to Francesco Sciortino, Giancarlo Ruocco, Paolo De Los Rios, Carlo Pierleoni, Giovanni Ciccotti, and Guido Caldarelli for helpful discussions. S. M. acknowledges the University of Rome "La Sapienza" for a research grant. P. L. and P. C. acknowledge a grant from the Italian Space Agency (ASI).

[1] W. Kauzmann, Adv. Prot. Chem. **14**, 1 (1959).
[2] G.W. Robinson and C. H. Cho, Biophys. J. **77**, 3311 (1999).
[3] P. L. Privalov, Crit. Rev. Biochem. Mol. Biol. **25**, 281 (1990).
[4] J. Zhang, X. Peng, A. Jonas, and J. Jonas, Biochemistry **34**, 8631 (1995).
[5] H. S. Ashbaugh, T. M. Truskett, and P. G. Debenedetti, J. Chem. Phys. **116**, 2907 (2002).
[6] K. Lum, D. Chandler, and J. D. Weeks, J. Phys. Chem. **103**, 4570 (1999).
[7] M. I. Marques, J. M. Borreguero, H. E. Stanley, and N.V. Dokholyan, Phys. Rev. Lett. **91**, 138103 (2003).
[8] N. Nandi and B. Bagchi, J. Phys. Chem. **101**, 10 954 (1997).
[9] G. R. Andersen, S. Thirup, L. L. Spremulli, and J. Nyborg, J. Mol. Biol. **297**, 421 (2000).
[10] S. Melchionna and S. Cozzini, The DLPROTEIN User Manual, 2001, University of Rome.
[11] A. D. MacKerell *et al.*, J. Phys. Chem. B **102**, 3586 (1998).
[12] W. L. Jorgensen *et al.*, J. Chem. Phys. **79**, 926 (1983).
[13] H. Hu, M. Elstner, and J. Hermans, Proteins **50**, 451 (2002).
[14] M.W. Mahoney and W. L. Jorgensen, J. Chem. Phys. **112**, 8910 (2000).
[15] B. Guillot, J. Mol. Liq. **101**, 219 (2002).
[16] L. Stella and S. Melchionna, J. Chem. Phys. **109**, 10 115 (1998).
[17] P.-L. Chau and A. J. Hardwick, Mol. Phys. **93**, 511 (1998).
[18] J. R. Errington and P. G. Debenedetti, Nature (London) **409**, 318 (2001).
[19] H. Frauenfelder *et al.*, Biochemistry **26**, 254 (1987).
[20] F. Demmel, W. Doster, W. Petry, and A. Schulte, Eur. Biophys. J. **26**, 327 (1997).